Molecular Therapy
Original Article

Potential clinical use of azacitidine and MEK inhibitor combination therapy in *PTPN11*-mutated juvenile myelomonocytic leukemia

Santhosh Kumar Pasupuleti,[1,8] Karen Chao,[2,7,8] Baskar Ramdas,[1] Rahul Kanumuri,[1] Lakshmi Reddy Palam,[1] Sheng Liu,[3] Jun Wan,[3] Colleen Annesley,[4] Mignon L. Loh,[4] Elliot Stieglitz,[5] Michael J. Burke,[2] and Reuben Kapur[1,6]

[1]Herman B. Wells Center for Pediatric Research, Department of Pediatrics, Indiana University School of Medicine, 1044 W. Walnut Street, R4-168, Indianapolis, IN 46202, USA; [2]Department of Pediatrics, Children's Wisconsin, Medical College of Wisconsin, Milwaukee, WI 53226, USA; [3]Department of Medical and Molecular Genetics, Indiana University School of Medicine, Indianapolis, IN 46202, USA; [4]Seattle Children's Hospital, Seattle, WA, USA; [5]Department of Pediatrics, Benioff Children's Hospital, Helen Diller Family Comprehensive Cancer Center, University of California, San Francisco, San Francisco, CA, USA; [6]Department of Microbiology & Immunology, Indiana University School of Medicine, 1044 W. Walnut Street, R4-168, Indianapolis, IN 46202, USA; [7]Stanford University School of Medicine, Lucile Packard Children's Hospital, Palo Alto, CA, USA

Juvenile myelomonocytic leukemia (JMML) is a rare myeloproliferative neoplasm of childhood. The molecular hallmark of JMML is hyperactivation of the Ras/MAPK pathway with the most common cause being mutations in the gene *PTPN11*, encoding the protein tyrosine phosphatase SHP2. Current strategies for treating JMML include using the hypomethylating agent, 5-azacitidine (5-Aza) or MEK inhibitors trametinib and PD0325901 (PD-901), but none of these are curative as monotherapy. Utilizing an *Shp2*$^{E76K/+}$ murine model of JMML, we show that the combination of 5-Aza and PD-901 modulates several hematologic abnormalities often seen in JMML patients, in part by reducing the burden of leukemic hematopoietic stem and progenitor cells (HSC/Ps). The reduced JMML features in drug-treated mice were associated with a decrease in p-MEK and p-ERK levels in *Shp2*$^{E76K/+}$ mice treated with the combination of 5-Aza and PD-901. RNA-sequencing analysis revealed a reduction in several RAS and MAPK signaling-related genes. Additionally, a decrease in the expression of genes associated with inflammation and myeloid leukemia was also observed in *Shp2*$^{E76K/+}$ mice treated with the combination of the two drugs. Finally, we report two patients with JMML and *PTPN11* mutations treated with 5-Aza, trametinib, and chemotherapy who experienced a clinical response because of the combination treatment.

INTRODUCTION

Juvenile myelomonocytic leukemia (JMML) is the most common myeloproliferative neoplasm (MPN) in childhood and is caused by excessive proliferation of myelomonocytes.[1,2] Mutations in RAS family members including *NF1*, *CBL*, *KRAS*, *NRAS*, *RRAS*, *RRAS2*, or *PTPN11* are identified in 90%–95% of patients.[3,4] Traditional cytotoxic chemotherapy is not curative for this highly aggressive leukemia, and long-term remissions are only achievable using allogeneic hematopoietic stem cell transplantation (HSCT). However, even with HSCT nearly 50% of patients will relapse and die of their disease.[5]

The mitogen-activated protein kinase (MAPK) signaling pathway (RAS/RAF/MEK/ERK) is essential for cell proliferation, differentiation, and survival and has been shown to be overactive in several cancers.[6] Prior studies have shown that the Ras/MAPK pathway is deregulated in JMML through genetic and epigenetic alterations.[3,7] Several Ras-driven malignancies have benefited from targeted therapies using MAP/ERK kinase 1 and 2 specific (MEK 1/2) inhibitors to block RAS/MAPK overactivation.[8] Specific to JMML, preclinical studies using *KRAS* and *NF1* mutant mice treated with the allosteric MEK inhibitor PD0325901 (PD-901) have shown reduction in spleen size and white blood cells (WBCs) with resolution of anemia and thrombocytopenia.[9,10] Trametinib, a commercially available MEK inhibitor, has also demonstrated activity in patients with relapsed/refractory JMML.[11] Additionally, the use of epigenetic modifying drugs, such as 5-azacitidine (5-Aza), has been shown to be effective in patients with both newly diagnosed and relapsed JMML.[12,13] However, because of the polyclonal nature of JMML disease, monotherapies are not curative. While monotherapy of 5-Aza is well tolerated in children with newly diagnosed JMML,[12] *PTPN11*-mutant-bearing high-risk JMML patients in the presence of 5-Aza show emergence of new mutations and/or expansion of pre-existing resistant subclones leading to relapse.[14] In general, combinations of active agents have traditionally been shown to result in higher response rates and improved long-term outcomes in several hematologic malignancies.[15,16] To this end, a recent study showed that 5-Aza, when

Received 13 September 2022; accepted 31 January 2023;
https://doi.org/10.1016/j.ymthe.2023.01.030.

[8]These authors contributed equally

Correspondence: Michael J. Burke, MD, Department of Pediatrics, Children's Wisconsin, Medical College of Wisconsin, Milwaukee, WI 53226, USA.
E-mail: mmburke@mcw.edu
Correspondence: Reuben Kapur, PhD, Herman B. Wells Center for Pediatric Research, Department of Pediatrics, Indiana University School of Medicine, 1044 W. Walnut Street, R4-168, Indianapolis, IN 46202, USA.
E-mail: rkapur@iu.edu

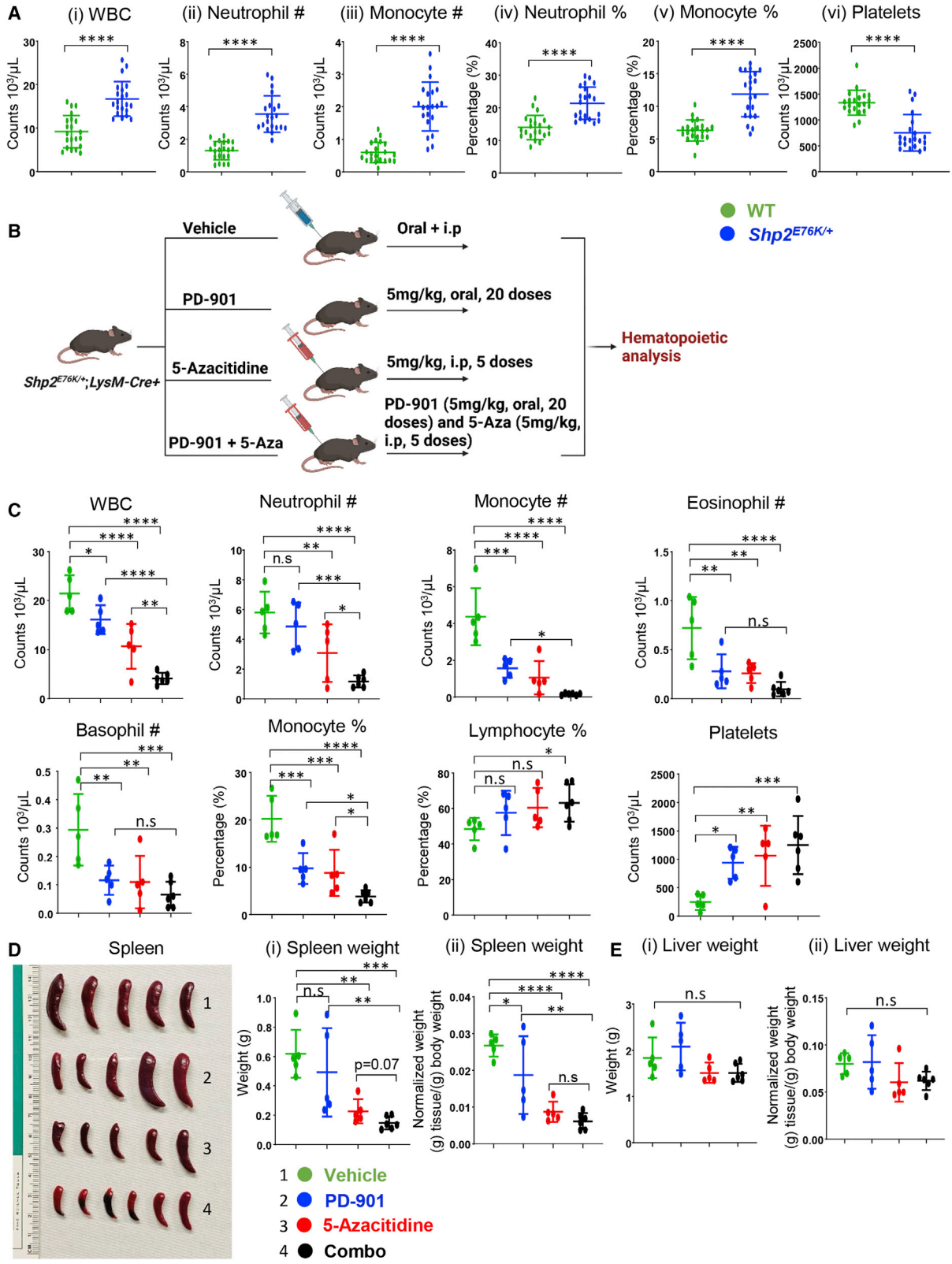

(legend on next page)

administered in combination with trametinib, prolonged the survival of mice in a model of chronic myelomonocytic leukemia (CMML) compared with monotherapy.[17] Furthermore, combination of 5-Aza and the MEK inhibitor trametinib also appears to show greater impact in a melanoma model.[18] Therefore, in the current study we assessed the efficacy of 5-Aza in combination with the MEK inhibitor PD-901 in a gain-of-function (GOF) *Shp2*$^{E76K/+}$ mouse model. We also report two *PTPN11*-mutated JMML patients who were treated with the combination of 5-Aza, trametinib, and chemotherapy, which resulted in a clinical response.

RESULTS

Combination of 5-azacitidine and MEK inhibitor PD0325901 regulates myeloproliferative neoplasia in *Shp2*$^{E76K/+}$ mice

We studied the impact of combined treatment with 5-Aza and PD-901 on JMML by utilizing a GOF *Shp2*$^{E76K/+}$ mutant mouse model. The primary *Shp2*$^{E76K/+}$ mutant mice (~13 weeks old, both males and females) develop features that are consistent with MPN, including increased peripheral blood (PB) WBCs, neutrophils, and monocyte counts, and decreased platelet counts compared with wild-type (WT) mice (Figure 1A). *Shp2*$^{E76K/+}$ mutant mice were randomized and treated with vehicle, 5-Aza, or PD-901, or a combination of both drugs (Figure 1B). After 4 weeks of drug treatment, all mice were sacrificed and analyzed for hematopoietic changes. The combination therapy (5-Aza + PD-901) improved JMML disease features including elevated WBCs, neutrophils, and monocytes and increased lymphocytes in the PB compared with other groups (Figure 1C). Importantly, the drug therapy decreased spleen size, a prominent feature in JMML, and partially reduced liver weight, although not significantly (Figures 1D and 1E). The combination therapy also reduced the number of leukemic myeloid cells (Gr-1$^+$/CD11b$^+$) and partially restored the monocytic skewing (increase in Gr1$^-$/CD11b$^+$ cells) in the PB (Figure 2A), bone marrow (BM), and spleens of *Shp2*$^{E76K/+}$ mice compared with other groups (Figures 2B and 2C). Furthermore, the frequency of myeloid blasts (c-KIT$^+$/CD11b$^+$ cells) in the spleens was also reduced in *Shp2*$^{E76K/+}$ mice after 4 weeks of combination therapy compared with other groups (Figure 2D).

To determine how 5-Aza and PD-901 combination therapy in *Shp2*$^{E76K/+}$ mice impacts the expansion of immature cells in the BM, we performed flow-cytometry analysis on BM cells. As seen in Figure 2E, combination therapy reduced the frequency of total Lin$^-$Sca1$^+$KIT$^+$ cells (LSK) as well as abnormal BM cellularity in *Shp2*$^{E76K/+}$ mice (Figure 2F). Moreover, the frequency of total and absolute number of hematopoietic progenitor-1 cells (HPC1; LSK/CD48$^+$/CD150$^-$) as well as long-term hematopoietic stem cells (LT-HSCs; LSK/CD48$^-$/CD150$^+$) was significantly reduced in *Shp2*$^{E76K/+}$ mice receiving combination therapy compared with the vehicle group (Figure 3A). To evaluate the impact of 5-Aza and PD-901 drug treatment on the presence of committed HSC/Ps, we assessed the frequencies and absolute numbers of common myeloid progenitors (CMPs), granulocyte macrophage progenitors (GMPs), megakaryocyte erythroid progenitors (MEPs), and common lymphoid progenitors (CLPs) in *Shp2*$^{E76K/+}$ mice. Combination therapy in the BM of *Shp2*$^{E76K/+}$ mice reduced the frequency and absolute number of CMPs (Lin−/c-KIT$^+$/CD16/32$^-$/CD34$^+$) and GMPs (Lin−/c-KIT$^+$/CD16/32$^+$/CD34$^+$) compared with other groups (Figure 3B). These findings demonstrate that the combination therapy of 5-Aza and MEK inhibitor can improve *Shp2*$^{E76K/+}$ mutant-driven HSC/P abnormalities to a different extent and in a cell-specific manner. As seen in Figures S1A–S1E, the combination treatment described above did not impact the hematopoietic content of WT mice.

Combination of 5-Aza and PD-901 treatment inhibits MEK/ERK signaling pathway in GOF *Shp2*$^{E76K/+}$ mutant HSC/Ps

To identify the impact on differentially expressed genes (DEGs) in *Shp2*$^{E76K/+}$ mice after 4 weeks of drug treatment, we performed RNA-sequencing (RNA-seq) studies on BM cells derived from vehicle- and drug-treated mice. Bioinformatics analyses revealed that a set of DEGs (1,681 genes) were downregulated and 1,218 genes were upregulated at a false discovery rate (FDR) of <0.05 between vehicle and combination therapy (Figure 4A). We assessed DEGs utilizing a scatterplot analysis (SPA) in which the lower-left quadrant represents genes that were downregulated in *Shp2*$^{E76K/+}$ mice treated with either 5-Aza or PD-901 (Figure 4B). The lower-left quadrant in Figure 4C represents a larger number of genes that were downregulated in *Shp2*$^{E76K/+}$ mice treated with combination therapy, including genes involved in pro-inflammatory monocyte/macrophage differentiation (*Cd14*),[19] inflammatory response (*Ccr5*),[20] tumor cell proliferation/progression (*Adam11*),[21] and MAPK superfamily (*Dusp6*).[22] Dual specificity phosphatase family (*DUSP*) genes regulate MAPK/ERK, JNK, p38 signaling, and AP1 transcription factors, which are associated with cell proliferation, apoptosis, and differentiation.[22] Elevated levels of *DUSP6* have been associated with disease progression and therapeutic resistance in patients with MPN.[23] Furthermore, higher expression of *DUSP6* in acute myeloid leukemia (AML) cells harboring *FLT3*^{ITD} mutation contribute to leukemic cell proliferation. In our hands, the expression of *Dusp* superfamily genes was reduced in the 5-Aza-treated *Shp2*$^{E76K/+}$ mutant group. *Dusp* gene expression was more profoundly downregulated in *Shp2*$^{E76K/+}$ mutant mice treated with the combination therapy (Figure 4D). Recent studies have suggested that the p38-MAPK/AP-1 signaling pathway is

Figure 1. Combination of 5-Aza and PD-901 drug treatment reduces myeloproliferative neoplasia in *Shp2*$^{E76K/+}$ mice

(A) (i) Total white blood cell (WBC) counts, (ii) neutrophil counts, (iii) monocyte counts, (iv) neutrophil percentages, (v) monocyte percentages, and (vi) platelet counts in peripheral blood of *Shp2*$^{E76K/+}$ or WT control mice. (n = ~21 mice per group). (B) Schematic of the *in vivo* drug treatment of *Shp2*$^{E76K/+}$ mice. (C) Peripheral blood counts at 4 weeks after indicated drug treatment in *Shp2*$^{E76K/+}$ mice. (D) Representative spleens of *Shp2*$^{E76K/+}$ mice treated with (1) vehicle, (2) PD-901, (3) 5-Aza, and (4) combination of 5-Aza + PD-901, with combination-treated *Shp2*$^{E76K/+}$ mice showing reduced splenomegaly, (i) quantification of spleen weights, and (ii) quantification of spleen weights normalized by body weights of *Shp2*$^{E76K/+}$ mice at 4 weeks after indicated drug treatment. (E) (i) Quantification of liver weights and (ii) quantification of liver weights normalized by body weights of *Shp2*$^{E76K/+}$ mice at 4 weeks after indicated drug treatment. (n = ~5–6 mice per group; *p < 0.05, **p < 0.005, ***p < 0.0005, ****p < 0.0001).

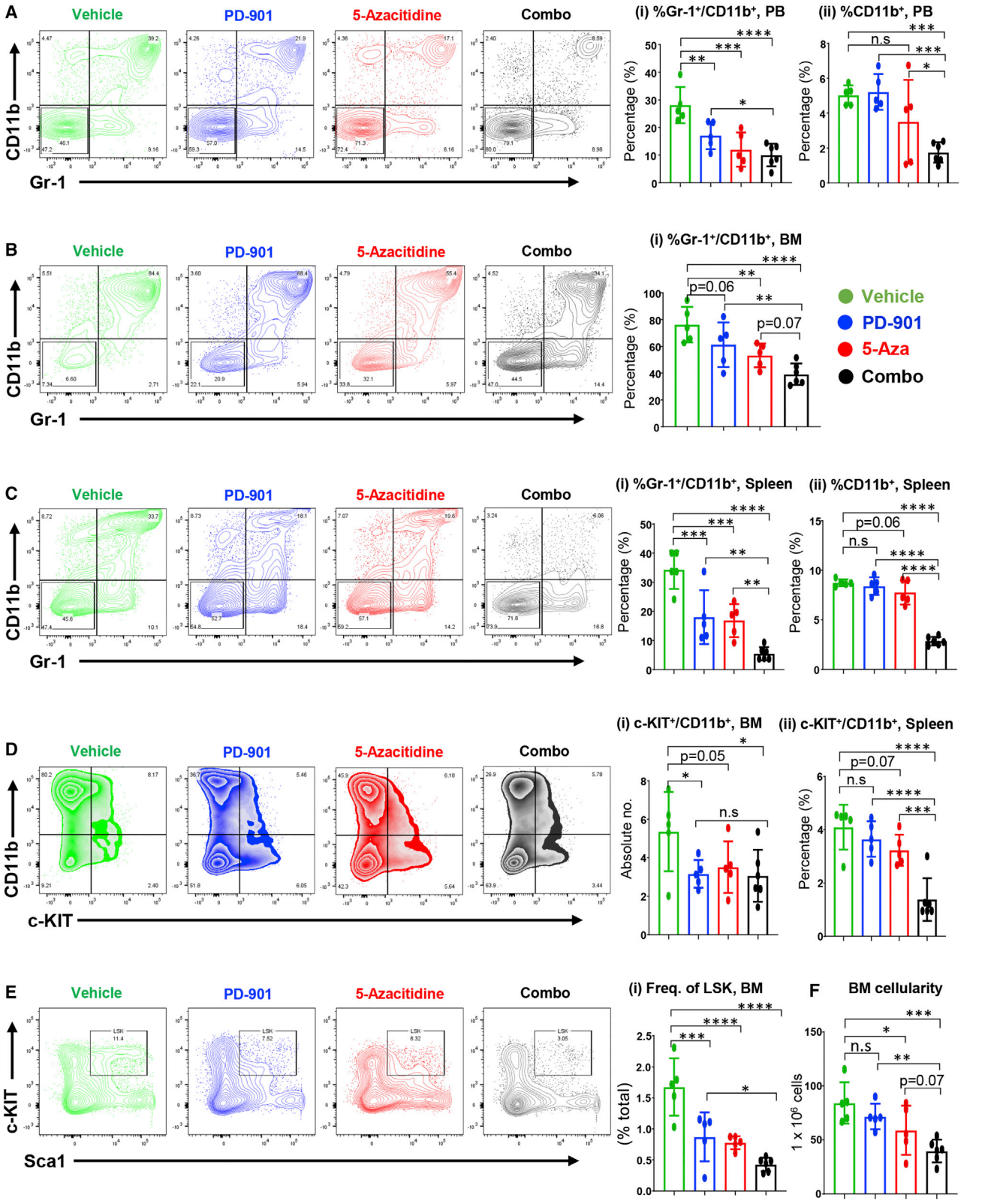

(legend on next page)

associated with drug resistance in patients with leukemia.[24] As seen in Figures 4E and 4F, the combination of 5-Aza and PD-901 treatment in *Shp2*$^{E76K/+}$ mice reduced the expression of genes related to p38-MAPK/AP-1 signaling compared with other groups.

Proteins encoded by the genes of the RAS signaling pathway play an important role in the transduction of extracellular signals to the nucleus and regulate cell proliferation and differentiation.[25] About 90%–95% of JMML patients have somatic mutations in the RAS signaling pathway, indicating that hyperactivation of the RAS signal plays a key role in the pathogenesis of JMML.[3,25] We hypothesized that 5-Aza and PD-901 drug treatment might modulate the hyperactivation of the RAS pathway in *Shp2*$^{E76K/+}$ mice. Consistently, the expression of genes related to the RAS pathway was partially decreased in the 5-Aza drug-treated group. Importantly, the combination of 5-Aza and PD-901 further reduced the expression of genes in the RAS pathway in *Shp2*$^{E76K/+}$ mice (Figure 4G). Next, we analyzed the expression of RAS downstream signaling, including MAPK and ERK1/2 signaling in 5-Aza and PD-901 drug-treated mice. Gene set enrichment analysis (GSEA) revealed that the combination of two drugs reduced the expression of MAPK and ERK1/2 signaling-related genes in *Shp2*$^{E76K/+}$ mice compared with other groups (Figures 4G and S2A). This decrease in the MAPK/ERK-related genes was associated with a reduction in the activation of MEK and ERK at the biochemical level in mice treated with combination therapy (Figure 4H).

Combination therapy is associated with partial restoration in the expression of several genes associated with inflammation, cytokine, and chemokine production in *Shp2*$^{E76K/+}$ mice

To analyze the impact of combination therapy on mutant BM cells, we further examined our bulk RNA-seq data obtained from BM cells. As seen Figure 4G, combination therapy in *Shp2*$^{E76K/+}$ mice was associated with downregulation in the expression of genes involved in inflammatory response as well as cytokine and chemokine production. Furthermore, GSEA analysis revealed a significant reduction in the number of inflammatory response-related genes in combined drug-treated *Shp2*$^{E76K/+}$ mice compared with other groups (Figure S2B). Consistent with these results, interleukin-6 (*IL-6*), which is a pro-inflammatory cytokine involved in promoting MAPK, phosphatidylinositol 3-kinase (PI3K)/Akt, and nuclear factor (NF)-κB signaling, and plays a key role in inflammation, immunosuppression, tumorigenesis, and drug resistance in cancer cells,[26] was downregulated in *Shp2*$^{E76K/+}$ mice treated either with 5-Aza or a combination of the two drugs (Figure S2Ci). Given that RNA-seq analysis was performed on bulk BM cells, it is difficult to say which specific cell type contributed to the reduction in these responses and whether the reduction in inflammatory cytokine production was due to a decrease in the cell type producing it or a result of reduction in its expression on an individual cell basis. Similarly, nuclear factor of κ light polypeptide gene enhancer in B cell inhibitor ζ (*Nfkbiz*), a member of the IκB family gene that interacts with *NF-κB* and controls the initiation of secondary response genes including *IL-6* and *IL-10*,[27,28] was reduced in 5-Aza and combined drug-treated mice (Figure S2Cii). *IL-15* is a pro-inflammatory cytokine, which binds to its receptor and activates the Jak1/Jak3/Stat5 signaling pathway.[29] *Il-15* was reduced in the combined drug treatment group (Figure S2Ciii). Furthermore, proline-serine-threonine phosphatase-interacting protein 1 (*Pstpip1*; also known as *Cd2bp1*), which is a cytoskeleton-associated adapter protein and is highly expressed in hematopoietic cells,[30] was downregulated in combined drug-treated mice (Figure 5Civ). *Pstpip1* binds PEST-type protein tyrosine phosphatases and modulates *c-Abl* and Fas ligand activity. It also regulates T cell activation and β cell release.[30] *Pstpip1* gene also interacts with pyrin, which is found in association with the cytoskeleton in myeloid and monocytic cells and controls immunoregulatory functions[30,31] (Figure S2Civ).

NLRP3 inflammasome promotes a chronic inflammatory response, which contributes to cancer initiation, development, and progression.[32] Higher expression of *Nlrp3* also promotes the progression of AML via the *IL-1β* signaling pathway.[33] We found a decrease in the expression of *Nlrp3* in 5-Aza- and combined-drug-treated mice (Figure S2Cv). Likewise, inflammatory chemokine (C-C motif) ligand 4 (*CCL4*), also known as macrophage inflammatory protein-1β, plays a key role in tumor development and progression by recruiting regulatory T cells and pro-tumorigenic macrophages. Elevated serum *CCL4* levels in patients with AML promote an inflammatory state and suppress cytotoxic T cells, and promote disease progression.[34] We found *Ccl4* levels to be downregulated in *Shp2*$^{E76K/+}$ mice treated with the combination of the two drugs (Figure S2Cvi).

Given the correction of myeloid cells in *Shp2*$^{E76K/+}$ mice treated with the combination of two drugs (Figures 1C and 2A–2C), we looked to assess whether this partial rescue was associated with downregulation of myeloid leukemia-related genes in the combined drug treatment group compared with other groups. As seen in Figure S2D, a decrease in the expression of several leukemia-associated genes was observed in the combined-drug-treated group, including the expression of *Mapk7*, *Tgfbr2*, *Csf1r*, *ApoE*, *Timp2*, and *Syk* (Figure S2Ei–vi).

Figure 2. Combination of 5-Aza and PD-901 drug treatment reduces leukemic myeloid cells in *Shp2*$^{E76K/+}$ mice

(A) Representative flow-cytometry profile of Gr-1$^+$/CD11b$^+$ myeloid cells in the PB of the indicated drug-treated mice, (i) frequency of Gr-1$^+$/CD11b$^+$ myeloid cells in PB, and (ii) frequency of CD11b$^+$ cells in PB at 4 weeks after indicated drug treatment. (B) Representative flow-cytometry profile of Gr-1$^+$/CD11b$^+$ myeloid cells in the BM of the indicated drug-treated mice, (i) frequency of Gr-1$^+$/CD11b$^+$ myeloid cells in BM at 4 weeks after indicated drug treatment. (C) Representative flow-cytometry profile of Gr-1$^+$/CD11b$^+$ myeloid cells in the spleens of the indicated drug-treated mice, (i) frequency of Gr-1$^+$/CD11b$^+$ myeloid cells in spleens, and (ii) frequency of CD11b$^+$ cells in spleens at 4 weeks after indicated drug treatment. (D) Representative flow-cytometry profiles of c-KIT$^+$/CD11b$^+$ myeloid blasts from the indicated drug-treated mice, (i) absolute number of c-KIT$^+$/CD11b$^+$ cells in the BM, and (ii) frequency of c-KIT$^+$/CD11b$^+$ cells in the spleens at 4 weeks after indicated drug treatment. (E and F) Representative flow-cytometry profile of LSK (Lin$^-$/Sca-1$^+$/c-KIT$^+$) cells in the BM from the indicated drug-treated mice, (i) frequency of total LSK cells in the BM, and (F) BM cellularity at 4 weeks after indicated drug treatment (n = ∼5–6 mice per group; *p < 0.05, **p < 0.005, ***p < 0.0005, ****p < 0.0001).

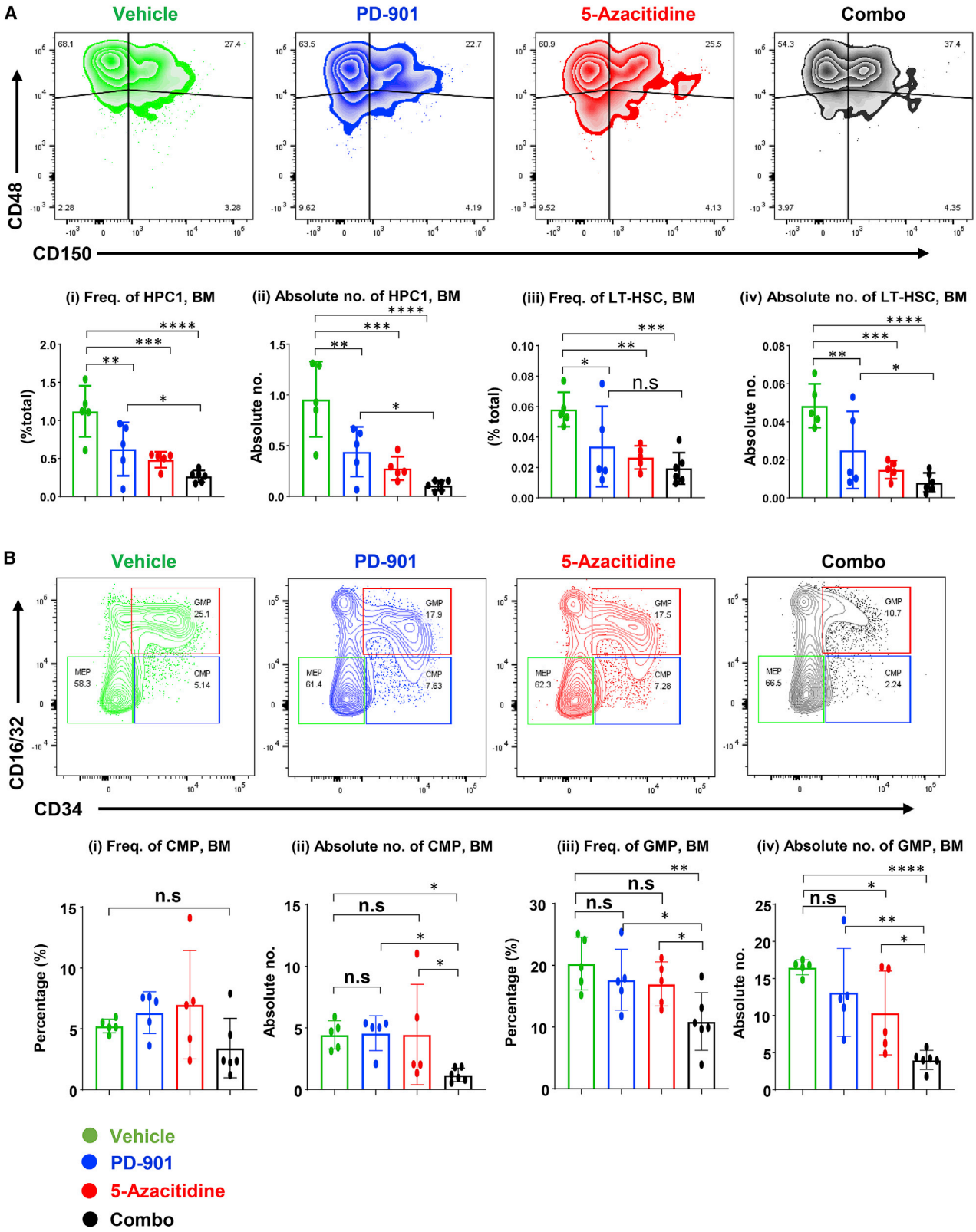

(legend on next page)

Combined drug treatment is associated with a decrease in integrin-mediated signaling genes and improves erythrocyte development-related genes in *Shp2*$^{E76K/+}$ mice

PTPN11 mutant HSC/Ps in JMML patients migrate to the spleen, liver, and lungs.[1] Given the reduced burden of these cells in these tissues, we hypothesized that combined drug treatment of 5-Aza and PD-901 might reduce the expression of genes involved in cell migration and invasion in *Shp2*$^{E76K/+}$ mice. To this end, expression of integrins in tumor cells contributes to tumor cell progression and metastasis as well as proliferation and survival.[35,36] Importantly, integrins play an important role in hematopoietic stem cell (HSC) maintenance, proliferation, and stemness in the BM niche.[37] RNA-seq analysis revealed that integrin signaling-related genes, including integrin β-2 (*Itgb2*), integrin β-5 (*Itgb5*), integrin α-8 (*Itga8*), integrin α-x (*Itgax*), *Cd9*, and Fc epsilon receptor Ig (*Fcer1g*) were all higher in *Shp2*$^{E76K/+}$ mice treated with vehicle, but treatment with the combination of 5-Aza and PD-901 reduced their expression (Figures 5A–5D). These results suggest that the combined drug treatment reduced the burden of leukemic cells in the BM as well as an associated increase in bulk integrin expression.

Apart from monocytosis and splenomegaly, patients with JMML often have anemia and thrombocytopenia.[38] In our study, we observed that the JMML mice had anemia and thrombocytopenia. As shown in Figure 1C, the combination of 5-Aza and PD-901 reversed the thrombocytopenia with improved platelet counts into the normal reference range. Furthermore, our Ingenuity Pathway Analysis (IPA) and DEG analysis showed that genes involved in erythrocyte and megakaryocyte development and differentiation were increased in the combined drug treatment group, including genes such as glycophorin A (*Gypa*), pleckstrin 2 (*Plek2*), GATA binding protein 1 (*Gata1*), hemoglobin subunit α2 (*Hba2*), TAL BHLH transcription factor 1 or erythroid differentiation factor (*Tal1*), SRY-Box transcription factor 6 (*Sox6*), Kruppel-like factor 1 (*Klf1*), and solute carrier family 11 member 2 (*Slc11a2*), compared with the other groups (Figures 6A–6C). These improvements in gene expression were associated with an increase in the frequency of MEP (c-KIT$^+$/CD16/32$^-$/CD34$^-$) population. As shown in Figures 3B and 6D, the combination of the two drugs improves the MEP population in *Shp2*$^{E76K/+}$ mice compared with the vehicle group or single-drug-treated group.

To assess the composition of various BM cells in mutant mice, as a result of combined drug treatment in *Shp2*$^{E76K/+}$ mice, including subsets of monocytes, macrophages, myeloid dendritic cells, neutrophils, T cells, and B cells, we conducted bulk BM RNA-seq analysis and performed deconvolution analysis with the immunedeconv R package[39] using TIMER[40] and mMCPCounter,[41] a computational method that enables inference of cell-type-specific gene expression profiles. As seen in Figures S3A and S3B, combination treatment with 5-Aza and PD-901 in *Shp2*$^{E76K/+}$ mice resulted in downregulation in the expression of genes involved in myeloid dendritic cells, macrophages, monocytes, and neutrophils compared with other groups, along with an increase in the expression of genes associated with CD8$^+$ T cells (Figure S3B).

Combined treatment of 5-Aza and MEK inhibitor improves JMML disease features in patients with *PTPN11* mutations

While our preclinical data in a mouse model of JMML showed significant improvement in JMML disease features after combined drug treatment, we sought to examine whether patients with JMML who were previously treated with 5-Aza and an MEK inhibitor (trametinib) would have similar findings. The first case was a female infant born with Noonan syndrome (NS) who was found to have normocytic anemia and thrombocytopenia shortly after birth. Genetic testing of her PB and buccal swabs revealed a heterozygous *PTPN11* C.227A>T (p.Glu76Val) mutation consistent with NS. The patient had classic stigmata of NS with facial dysmorphism and pulmonary stenosis, and was later identified to have developmental delay. This was a *de novo* mutation, as her family history did not reveal any members with NS. At 6 months of age, she met criteria for JMML associated with NS with an absolute monocytosis (4.28×10^9/L), absence of the Philadelphia chromosome with 3.8% aberrant myeloblasts by flow cytometry in the BM, and splenomegaly. Additionally she had an elevated fetal hemoglobin (18.3 g/dL) for age, thrombocytopenia, and early myeloid precursors in the PB. At 9 months of age, given her persistent and symptomatic thrombocytopenia along with the presence of peripheral blasts, she began treatment with 5-Aza (75 mg/m^2/dose) given for 5 days on a 28-day cycle. She received a total of three cycles of 5-Aza, after which her need for platelet transfusions improved from twice a week to weekly. By 1 year of life, her platelet transfusion need decreased as infrequently as every 7 months, but her platelet count remained low. Her JMML continued to be managed with supportive care only, with the idea that it might resolve on its own given its association with NS. However, at 2 years of age the patient presented with respiratory syncytial virus bronchiolitis requiring hospitalization, and quickly progressed to acute respiratory distress syndrome with respiratory failure and recurrence of peripheral blasts. She developed progressive hepatosplenomegaly, and a BM evaluation showed 3% abnormal myeloblasts with a new cytogenetic abnormality of a ringed chromosome 18, but no morphologic evidence of transformation to AML. Because of her progressive respiratory failure, she was intubated but failed a conventional ventilator and was moved to an oscillator. A repeat BM aspirate at this time identified transformation of her JMML to AML with now 26% abnormal

Figure 3. Combination of 5-Aza and PD-901 drug treatment reduces leukemic HSC/Ps in *Shp2*$^{E76K/+}$ mice

(A) Representative flow-cytometry profile of CD48 and CD150 expression in leukemic LSK cells in the BM from the indicated drug-treated mice, (i) frequency of total and (ii) absolute number of LSK/CD48$^+$/CD150$^-$ LSK cells (HPC1), (iii) frequency of total LT-HSCs (LSK/CD48$^-$/CD150$^+$ cells), and (iv) absolute number of LT-HSCs in the BM at 4 weeks after indicated drug treatment. (B) Representative flow-cytometry profile of committed progenitors in the BM, (i) frequency and (ii) absolute number of common myeloid progenitors (CMPs; Lin$^-$/c-KIT$^+$/CD16/32$^-$/CD34$^+$ cells), (iii) frequency, and (iv) absolute number of granulocyte macrophage progenitors (GMPs; Lin$^-$/c-KIT$^+$/CD16/32$^+$/CD34$^+$ cells) in the BM at 4 weeks after indicated drug treatment (n = ~5–6 mice per group; *p < 0.05, **p < 0.005, ***p < 0.0005, ****p < 0.0001).

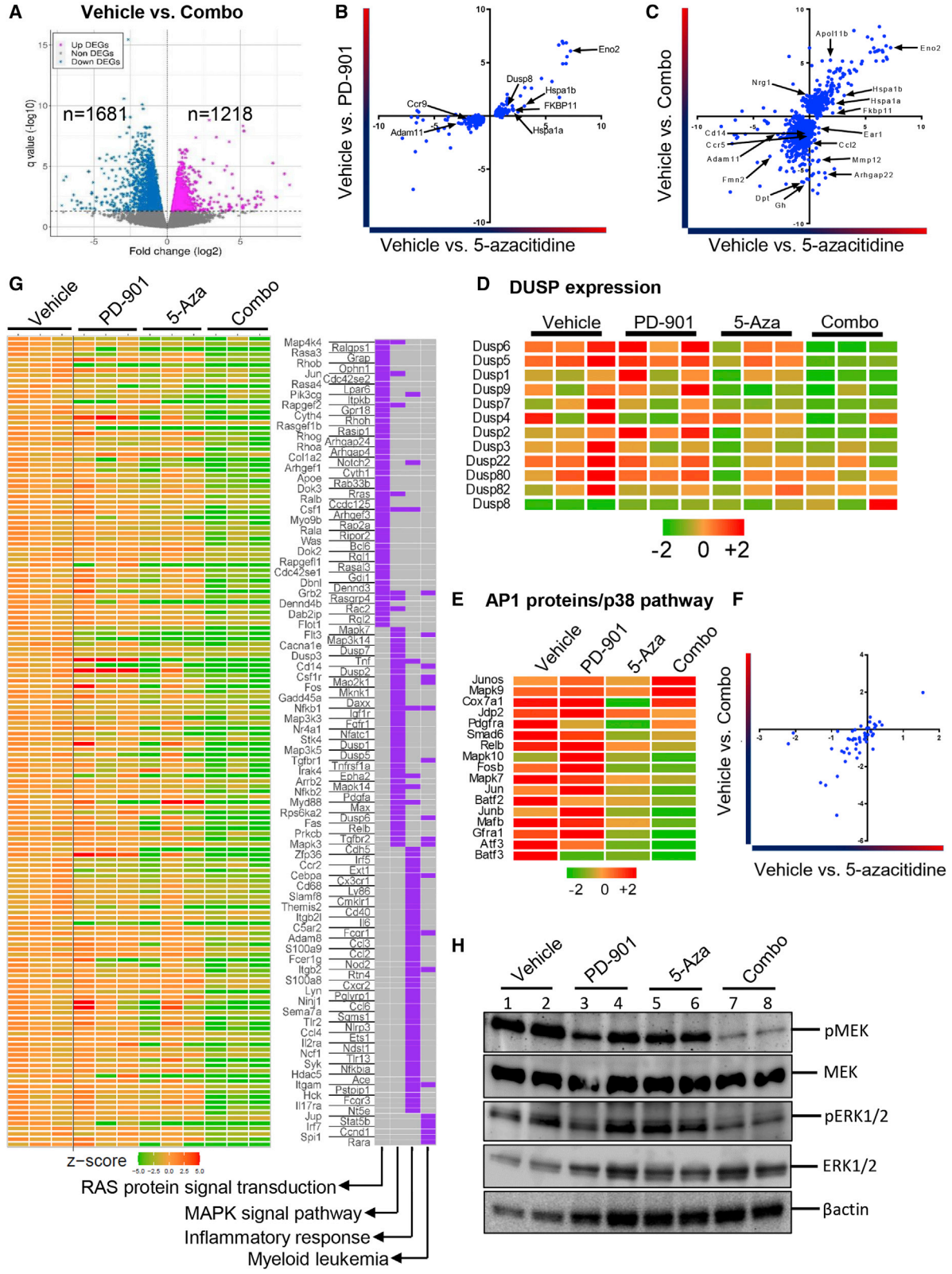

(legend on next page)

myeloblasts. Given the severity of the disease and after parental informed consent was given, the patient was treated with the combination of 5-Aza (days 1–5), trametinib (days 1–28), cytarabine (days 6–10), and fludarabine (days 6–10). Within 2 days of starting treatment with just 5-Aza and trametinib, the patient experienced a dramatic improvement in her splenomegaly and had a marked decrease of her lactate dehydrogenase (>13,000 to 5,936) and WBC count (70,000 to 39,500). Before starting fludarabine and cytarabine, the patient's spleen size reduced from 12 cm to 3 cm and her peripheral blast count reduced from 20% to 5%. Within 2 weeks of receiving this therapy, the patient had complete resolution of her hepatosplenomegaly, normalization of all abnormal laboratory values. She was extubated from the ventilator and was successfully taken off all supplemental oxygen (Table 1). Overall the combination of 5-Aza, trametinib, and chemotherapy was well tolerated, as the patient had no serious adverse events. A follow-up BM evaluation at the end of the treatment cycle reported a partial response with 8.6% abnormal myeloblasts. Given the persistent disease and overall poor predicted outcome of this diagnosis, the parents chose to pursue palliative care rather than further chemotherapy, and the patient passed away at home a few months later.

In the second case, a 4-year-old boy with no significant medical history presented with several days of abdominal distension and fever. Abdominal ultrasound revealed marked hepatosplenomegaly, and labs were notable for a WBC count of 22×10^9/L, an absolute monocyte count of 1.2×10^9/L, 6% circulating blasts, and a platelet count of 46×10^9/L. BM evaluation revealed a hypercellular marrow with evidence of myeloid dysplasia, absence of the Philadelphia chromosome, and 7% myeloblasts by flow cytometry. The patient clinically worsened, requiring admission to the intensive care unit for tachypnea and hypoxemia. He was started on treatment with 5-Aza, fludarabine, and cytarabine for a presumed aggressive myeloid neoplasm not yet elucidated. On day 3 of a planned 5-day course, the patient experienced a rapid clinical deterioration with hypoxemic respiratory failure, requiring extracorporeal life support (ECLS) and continuous renal replacement therapy (CRRT); therefore days 4 and 5 of chemotherapy were omitted. During this time, hemoglobin F resulted as markedly elevated at 63.8%. The patient's Oncoplex (cancer gene panel) results from the BM revealed multiple mutations consistent with a diagnosis of JMML including *PTPN11* C.227A>T (p.Glu76Val) with a variant allele frequency (VAF) of 66%, *NF1* C.2033dup (VAF 17%), an insertion of 62 bp in the SH2 domain of *SH2B3*, and *MYB* p.I376Sfs*6 (VAF 12%). Given the patient's clinical status and inability to resume intensive chemotherapy, he began trametinib monotherapy on day 12 after his initial treatment. The patient was removed from ECLS on day 13. Owing to concern for inadequate disease control with a rising monocyte count to 2.05×10^9/L, 5-Aza was added to trametinib (days 18–22). CRRT was discontinued on day 29, and a BM evaluation performed on day 40 demonstrated a residual abnormal myeloblast population of 0.6% by flow cytometry and a decrease in *PTPN11* VAF to 31.98%. The patient continued on trametinib until this BM evaluation (days 12–40), although he subsequently developed abdominal pain and trametinib was held for 5 days prior to starting the next chemotherapy course.

Six days following this marrow evaluation, the patient began his second cycle of 5-Aza, fludarabine, and cytarabine (days 1–5), and restarted trametinib. However, trametinib was held on day 3 of chemotherapy because of the recurrence of abdominal pain, distention, and diarrhea. During this time the patient also developed cytarabine syndrome requiring dexamethasone and experienced feeding intolerance needing parenteral nutrition. Imaging revealed moderate dilation of the entire colon without signs of infection, ultimately believed to be sequelae of ECLS, and slowly improved over time. Trametinib was restarted on day 10 of this cycle at 75% dosing, then increased to 100% dosing on day 23 with improved tolerance and no further holds needed. A BM evaluation on day 43 of this cycle demonstrated an abnormal myeloid blast population by flow cytometry that was below the limit of detection at <0.01%, and *PTPN11* VAF was negative with a limit of detection of <1%, consistent with molecular remission. The patient remained on trametinib, and 8 days following this marrow evaluation he began a 7-day course of 5-Aza. Three weeks following the start of this course, the patient underwent BM evaluation that showed no detectable minimal residual disease by flow cytometry and ongoing negative *PTPN11* at <1% (Table 2). Two weeks following this BM valuation a second course of 5-Aza for 7 days was initiated for the patient, intended as bridging therapy prior to HSCT. At the time of this report the patient remains on trametinib, tolerating it well with no significant side effects. The patient continues to have significant splenomegaly with only a marginal decrease in his spleen size, but his platelet count is now within normal range at $>150 \times 10^9$/L. He is doing well as an outpatient, on trametinib and awaiting the start of conditioning therapy for a matched unrelated donor HSCT. Of note, this patient was negative for a germline *PTPN11* mutation using cultured skin fibroblasts.

Figure 4. RNA-seq and western blot analysis revealed downregulation in the expression of MEK/ERK signaling pathway in combined drug-treated *Shp2*$^{E76K/+}$ mice

(A) Volcano plot showing fold change and FDR adjusted p value in response to combination therapy in *Shp2*$^{E76K/+}$ mice. (B) Scatterplot analysis (SPA) of differentially expressed genes (DEGs) in either 5-Aza or PD-901 drug treatment group. Lower-left quadrant: genes downregulated in 5-Aza and PD-901 drug treatment group. Top-left quadrant: genes upregulated in PD-901 drug treatment group but downregulated in 5-Aza drug treatment group. Lower-right quadrant: genes downregulated in PD-901 group but upregulated in 5-Aza drug treatment group. Top-right quadrant: genes upregulated in 5-Aza and PD-901 drug treatment group. (C) SPA of DEGs in combination of 5-Aza and PD-901 drug treatment. (D) Heatmap of *Dusp* family genes in *Shp2*$^{E76K/+}$ mice treated with indicated drug treatment. (E and F) Heatmap (E) and SPA analysis (F) of Ap1 proteins or p38 pathway genes in *Shp2*$^{E76K/+}$ mice treated with indicated drug treatment. (G) Heatmap of downregulated genes associated with RAS protein signal transduction, MAPK signaling pathway, inflammatory response, and myeloid leukemia in indicated drug treatment group. If a gene is in a particular pathway, it is marked purple in the right-hand panel. (H) BM cells from drug-treated *Shp2*$^{E76K/+}$ mice subjected to western blot analysis using antibodies against the indicated proteins.

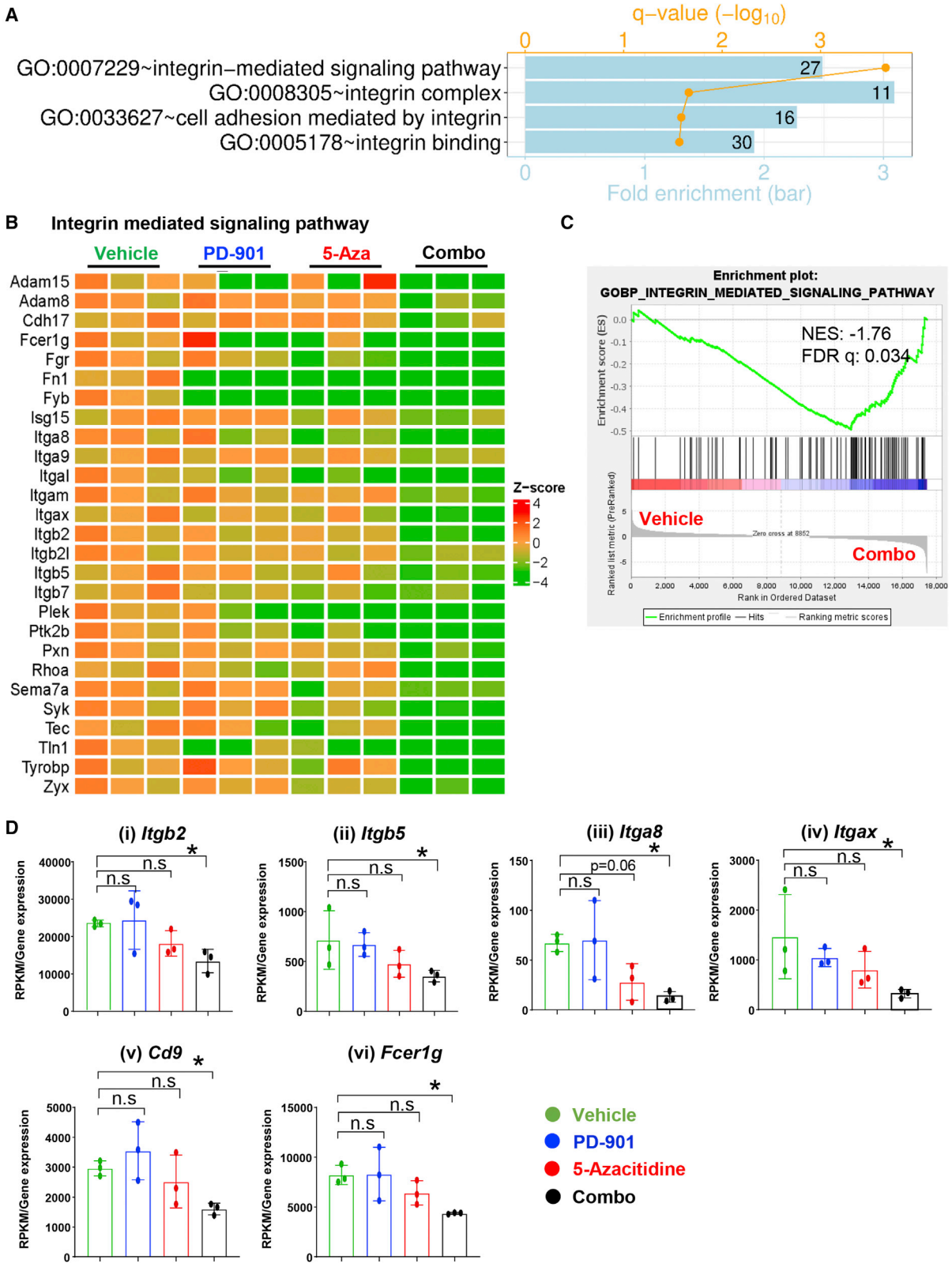

(legend on next page)

DISCUSSION

JMML is a severe MPN that affects infants and young children. Standard cytotoxic chemotherapy is ineffective in JMML patients.[42] The only curative treatment is myeloablation followed by HSCT; however, even with this rigorous therapy, 50% of patients relapse with leukemia and a second transplant only rescues one-third of patients.[5] Thirty-five percent of JMML cases have somatic activating mutations in *PTPN11*, which encodes the protein tyrosine phosphatase SHP2 and leads to hyperactive Ras signaling.[43] RAS proteins function as guanine nucleotide-regulated on-off switches to control a variety of cellular processes that drive cell growth and survival. Normally, Ras proteins function as molecular switches by cycling between active guanosine triphosphate-bound and inactive guanosine diphosphate-bound conformations, which then binds to a variety of effector proteins to activate downstream signaling cascades including RAF/MEK/ERK MAPK and PI3K/AKT pathways. Because of its important role in regulating cell growth and survival, RAS signaling is often exploited by cancer cells to proliferate without the need for external stimuli.[44] As direct targeting of oncogenic RAS has been difficult with small-molecule inhibitors, studies have focused on inhibiting the RAS downstream molecules including MAPK and PI3K. MEK inhibitors have shown some effect, but responses have not been durable.[44]

PD-901, a potent and selective allosteric MEK inhibitor, has been used in preclinical studies involving *KRAS* and *NF1* mutant mice. Treatment of these mice with PD-901 results in reduction in spleen size and WBCs along with resolution of anemia and thrombocytopenia.[9,10] Trametinib is a highly selective allosteric inhibitor of MEK1/2 with good oral bioavailability. Trametinib was the first MEK inhibitor approved by the Food and Drug Administration for treatment of melanoma.[45] In a preclinical study, trametinib treatment showed high efficacy in colorectal cancer xenograft models.[46] Furthermore, studies showed that trametinib effectively reduces the growth of RAS-mutant-bearing infant acute lymphoblastic leukemia cells *in vitro* and *in vivo*.[47,48] Importantly, trametinib treatment has also demonstrated activity in patients with relapsed/refractory JMML.[11] Additionally, the use of epigenetic modifying drugs, such as 5-Aza, show effectiveness in patients with both newly diagnosed and relapsed JMML.[12,13] Because of the polyclonal nature of JMML disease, monotherapies are not curative. One strategy to improve the efficiency of MAPK-targeting drugs is to combine them with other drugs. JMML patients, who receive a combination of trametinib and chemotherapeutic regimens, including cytarabine, never achieve complete remission.[49] However, Kloos et al. showed that 5-Aza, when administered in combination with trametinib, prolongs the survival of mice with CMML when compared with monotherapy.[17]

The treatment of JMML is still reliant on HSCT in the majority of patients. Two targeted strategies that have recently been prospectively evaluated in this disease include 5-Aza and MEK inhibition. In this study, we evaluated combining these approaches in a preclinical model. We specifically demonstrate a reduction in some of the HSC/P subsets in the combination therapy arm versus either arm alone, which is critical because in the $Shp2^{E76K}$ JMML model HSC/Ps represent disease-initiating cells.[50] Our findings suggest that the combination of 5-Aza and PD-901 impairs the hyperproliferation of immature myeloid cells in $Sph2^{E76K/+}$ mutant mice. Importantly, we observed that the combination of these drugs is well tolerated in normal WT mice. Furthermore, our RNA-seq analysis revealed that a larger number of genes that were downregulated in $Shp2^{E76K/+}$ mice treated with the combination therapy included genes involved in pro-inflammation and MAPK/DUSP genes including *Dusp6*, which dephosphorylates ERK1/2 to negatively regulate ERK signaling and plays an important role in chemotherapy resistance. *DUSP*s also regulate MAPK/ERK, JNK, p38 signaling, and AP1 transcription factors, which are associated with cell proliferation, apoptosis, and differentiation.[22] Higher expression of *DUSP6* in AML cells harboring $FLT3^{ITD}$ mutation contributes to leukemic cell proliferation.[51] Tumor cell resistance in both solid cancers and leukemia is closely associated with higher expression of *DUSP*s.[52,53] Furthermore, elevated levels of *DUSP6* is associated with disease progression and therapeutic resistance in patients with MPN.[23] Higher expression of *DUSP*s results in greater chemotherapeutic resistance of tumor cells.[54] Conversely, reduced *DUSP* activity leads to reduced chemotherapeutic resistance in tumors.[55] In our study, *Dusp* gene expression was more profoundly downregulated in $Shp2^{E76K/+}$ mutant mice treated with the combination of 5-Aza and PD-901 therapy. Recent studies have suggested that the p38-MAPK/AP-1 signaling pathway is associated with drug resistance in patients with leukemia.[24] We show that the combination of 5-Aza and PD-901 treatment in $Shp2^{E76K/+}$ mice significantly reduces the expression of genes related to p38-MAPK/AP-1 signaling.

We also describe the first two patients to receive the combination of 5-Aza, trametinib, and chemotherapy. This combination therapy was well tolerated in these critically ill patients, was effective at reducing the spleen size and blast counts, and allowed the patients to be extubated and leave the hospital. Taken together, our findings suggest that the combination of 5-Aza and MEK inhibition improves JMML disease features in $Shp2^{E76K/+}$ mutant mice as well as in two patients with *PTPN11*-mutated JMML. The combination of 5-Aza, trametinib, and chemotherapy for newly diagnosed patients with JMML is currently in development as a clinical trial.

MATERIALS AND METHODS

Mice

All mice were bred and maintained under specified pathogen-free conditions in the animal facility at Indiana University School of Medicine with 12:12-h light/dark cycle and were provided food

Figure 5. Combined drug treatment reduces expression of genes associated with integrin signaling in $Shp2^{E76K/+}$ mice

(A) IPA of genes associated with integrin signaling showed significant downregulation in combined drug treatment group. (B and C) Heatmap (B) and GSEA analysis (C) showing DEGs related to integrin-mediated signaling in response to individual and combination therapy in $Shp2^{E76K/+}$ mice. (D) Quantitative gene expression changes in response to individual and combined drug treatment in $Shp2^{E76K/+}$ mice. n = 3 mice per group, $^*p < 0.05$.

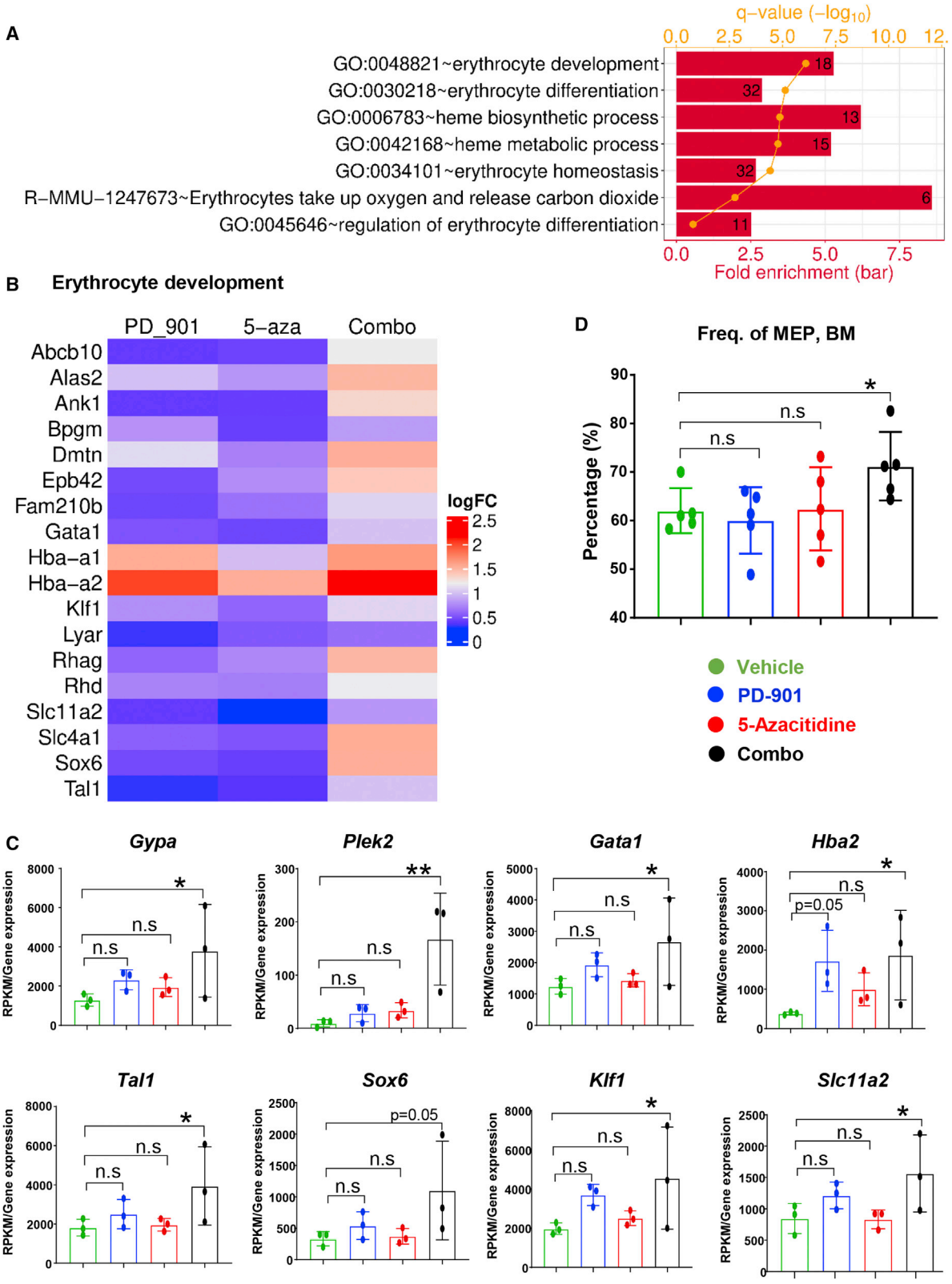

(legend on next page)

Table 1. Clinical characteristics of *PTPN11*-mutated JMML patient (case #1) upon combination of 5-Aza and MEK inhibitor treatment

Treatment day	Respiratory status	Liver/spleen (cm)	LDH (IU/L)	WBC (**10^3**/uL)	Blasts (%)
−1	conventional	4/12	10,052	41.4	14.0
0	oscillator	4/12	11,377	35.8	20.0
1	oscillator	3/7	7,453	22.5	13.0
2	oscillator	4/5	4,210	13.7	11.0
3	oscillator	–/4	3,355	18.3	10.0
4	oscillator	4/5	3,066	12.7	5.0
5	oscillator	4/5	2,970	24.5	4.0
10	conventional (day 6)/extubated	2/3	1,636 (normalized day 16)	0.6	0 (blasts undetectable by day 8)
28	room air	3/3	–	0.9	0

LDH, lactate dehydrogenase; WBC, white blood cell count.

and water *ad libitum*. All the animal experiments were approved and maintained by Laboratory Animal Resource Center at Indiana University School of Medicine. The $Shp2^{E76K/+}$;*LysM-Cre*$^{+}$ (GOF $Shp2^{E76K/+}$) mice have been described[50,56] and were identified by genotyping genomic DNA from tail snips. C57BL/6 mice were procured from Indiana University School of Medicine core facility and used as WT controls (both the GOF $Shp2^{E76K/+}$ and WT mice were age matched ∼13 weeks old, and both males and females were used in this study).

In vivo MEK inhibition in combination with 5-Aza

The GOF $Shp2^{E76K/+}$ mice were randomly assigned to cohorts that received either single or combination of PD-901 (5 mg/kg, via oral gavage for 5 days per week for 4 consecutive weeks for a total of 20 doses in 4 weeks) and 5-Aza (5 mg/kg, via intraperitoneal injection for 5 days given every other day per 4 weeks for a total of five doses in 4 weeks). Mice were harvested after 20 doses of PD0325901 and five doses of 5-Aza treatment.

Flow-cytometry analysis

Flow cytometry was performed as previously described.[50,57] For mature myeloid cell staining, freshly isolated PB, BM cells, and splenocytes were incubated with CD11b-PE, Gr-1-APC/Cy7, CD3-PE/Cy7, and B220-PerCp/Cy5.5. For HSC staining, Lin-PE cocktail (TER-119, Gr1, CD11b, B220, and CD3), c-Kit-APC, Sca-1-PE/Cy7, CD48-APC/Cy7, and CD150-PerCp/Cy5.5 were used. Similarly, for progenitor cell (CMP/GMP/MEP/CLP) staining, a panel of antibodies containing Lin-PE cocktail, c-Kit-APC/Cy7, Sca-1-PerCp/Cy5.5, CD16/32-PE/Cy7, CD34-BV421, and CD127-APC was used. A panel of antibodies containing c-Kit-APC and CD11b-PE was used for myeloid blast cell staining. Multiparameter flow-cytometric analysis was performed using an LSRFortessa flow cytometer with diva software (BD Biosciences), and the data were analyzed using FlowJo software (v10.7.0).[50,57]

Peripheral blood counts

PB counts in freshly collected mouse blood were performed using a hematology cell counter (HT5 Element).

Western blotting

Protein extracts were obtained from $Shp2^{E76K/+}$ drug-treated mice BM samples using ice-cold lysis buffer supplemented with protease and phosphatase inhibitors. An equal amount of protein extracts was separated on 4%–20% SDS-polyacrylamide gels. After electrophoresis, the proteins were transferred onto nitrocellulose membranes (NCMs), and nonspecific binding was blocked with 5% nonfat dry milk in Tris-buffered saline containing 0.1% Tween 20 (TBS-T). Membranes were then probed with various antibodies overnight at 4°C. After incubation, membranes were washed with TBS-T and incubated with appropriate horseradish peroxidase-conjugated secondary antibodies for 1 h at room temperature. After washing the membranes with TBS-T, the proteins on the membranes were detected using Clarity Max Western ECL substrate (Bio-Rad).

RNA sequencing, differential gene expression, and pathway enrichment analysis

RNA was extracted from single-cell suspension of $Shp2^{E76K/+}$ drug-treated mice BM cells in RLT buffer (lysis buffer for lysing cells and tissues prior to RNA isolation) using the RNeasy Plus Micro Kit (Qiagen) as per manufacturer's instructions. The RNA samples were processed and sequenced at Novogene as per manufacturer's instructions. The RNA-seq reads were mapped to the mouse genome mm10 using a STAR (v2.7.2a)[58] RNA-seq aligner with the

Figure 6. Combined drug treatment upregulates the expression of genes associated with erythrocyte/megakaryocyte development in $Shp2^{E76K/+}$ mice

(A and B) IPA (A) and heatmap (B) of $\log_2$ fold change (logFC) of genes associated with erythrocyte development were significantly upregulated in combined drug treatment group. (C) Quantitative gene expression associated with erythrocyte and megakaryocyte development in response to individual and combined drug treatment in $Shp2^{E76K/+}$ mice. n = 3 mice per group, *$p < 0.05$, **$p < 0.005$. (D) Frequency of megakaryocyte erythroid progenitors (MEPs; Lin^{-}/c-KIT^{+}/$CD16/32^{-}$/$CD34^{-}$ cells) in the BM at 4 weeks after indicated drug treatment (n = ∼5–6 mice per group; *$p < 0.05$).

Table 2. Clinical characteristics of *PTPN11*-mutated JMML patient (case #2; courses 1–4) upon combination of 5-Aza and MEK inhibitor treatment

Treatment day	Respiratory status	Spleen size (cm) (on US)	WBC (K/mm^3)	Blasts in PB/BM (%)	Platelets (K/mm^3)	AMC ($/mm^3$)	*PTPN11*-mutant VAF in BM (%)
Course #1							
−1	2 L O_2 NC	20.3	34.4	11/7	24	2,217	66
1	4 L O_2 NC	–	30.2	16%/–	25	3,020	–
2	BiPAP → intubated	16	30.7	7/–	27	10,131	–
3	V-V ECLS	–	16.5	12/–	87 (tx)	1,815	–
4	–	–	5.9	2/–	20	413	–
12	–	–	<0.2	0/–	19	0	–
13	off ECLS	–	<0.2	–	16	0	–
14	extubated → HFNC	–	0.2	–	6	0	–
18	HFNC	–	2.0	–	<5	1,298	–
22	HFNC	–	1.5	–	6	273	–
29	HFNC	19.5 (CT)	0.8	–	6	56	–
40	2 L O_2 NC	20.9	1.6	0/0.6	71	98	31.98
Course #2							
46/1 (4/11)	2 L O_2 NC	20.9	1.0	–	38	113	–
5	2 L O_2 NC	–	1.2	–	30	84	–
6 (4/16)	2 L O_2 NC	–	1.3	–	29	66	–
10	intermittent NC	–	0.8	–	10	0	–
11 (4/21)	intermittent NC	–	<0.2	–	9	0	–
43 (5/24)	room air	–	0.9	detected <0.01%	56	342	negative (LOD 1%)
Course #3							
51/1 (6/1)	room air	17 (CT)	2.5	–	80	333	–
7	room air		2.4	–	126	334	–
22 (6/22)	room air	15.2	1.8	negative	126	218	negative
Course #4							
36/1 (7/6)	room air	–	2	–	127	246	–
7	room air	–	2	–	152	178	–
28	room air	12.8	1.9	–	205	112	–

BiPAP, bilevel positive airway pressure; V-V, venovenous; NC, nasal cannula; ECLS, extracorporeal life support; HFNC, high-flow NC; US, ultrasound; CT, computed tomography; WBC, white blood cell count; AMC, absolute monocyte count; K, thousands; tx, transfused; PB, peripheral blood; BM, bone marrow; VAF, variant allele frequency; LOD, limit of detection.

following parameter: "–outSAMmapqUnique 60." Uniquely mapped sequencing reads were assigned to GENCODE M22 gene using featureCounts (v2.0.1)[59] with the following parameter: "-s 0 -p -Q 10 -O." The data were filtered using read count >10 in at least three of the samples, normalized using the TMM (trimmed mean of M values) method and subjected to differential expression analysis using edgeR (v3.38.4).[60,61] Gene ontology and pathway functional analysis was performed on differential expression gene with FDR cutoff of 0.05 using DAVID.[62,63] Furthermore, $\log_2$ fold change of gene expression between Combo and Vehicle were used for GSEA (version 4.1.0)[64] on selected pathways. The RNA-seq raw data were submitted to the NCBI Gene Expression Omnibus database (accession number GEO: GSE211278).

Deconvolution analysis

Deconvolution of bulk RNA-seq samples of $Shp2^{E76K/+}$ drug-treated mice was performed with the immunedeconv R package[39] using TIMER[40] and mMCPCounter[41] methods. The scores generated were visualized using Heatmap.

Statistics

Data were analyzed with Prism7 software (GraphPad). One-way ANOVA with uncorrected Fisher's test for multiple comparisons and Student's t test were used between two groups to evaluate statistical significance. p values of <0.05 were considered statistically significant (in figures: *$p < 0.05$; **$p < 0.005$; ***$p < 0.0005$; ****$p < 0.0001$; NS, not statistically significant).

DATA AVAILABILITY

The data that support the findings of this study are available from the corresponding author on reasonable request.

SUPPLEMENTAL INFORMATION

Supplemental information can be found online at https://doi.org/10.1016/j.ymthe.2023.01.030.

ACKNOWLEDGMENTS

The mouse protocol was approved by the Indiana University Laboratory Animal Resource Center, and all experiments were conducted at the Laboratory Animal Resource Center as per the protocol. Informed consent was obtained from the JMML patients who participated in this study. We thank our colleagues for technical support, critically reading our manuscript, and their suggestions to improve the manuscript. We would also like to thank Ms. Tracy Winkle for her administrative support. This work was supported by NIH grants R01CA173852, R01CA134777, R01HL146137, and R01HL140961, and Riley Children's Foundation (to R.K.). This work was also supported by the National Institutes of Health, National Cancer Institute grants 1U54CA196519 (E.S., M.L.L.) and the V Foundation (E.S.).

AUTHOR CONTRIBUTIONS

S.K.P., E.S., and R. Kapur conceived the study and designed experiments. S.K.P. executed the experiments and analyzed the data. K.C., M.J.B., C.A., and M.L.L. provided *PTPN11*-mutated JMML patients' clinical data. L.R.P., S.L., and J.W. analyzed the RNA-seq data. B.R. and R. Kanumuri assisted with the experiments. S.K.P., R.K., E.S., K.C., M.J.B., and C.A. wrote the manuscript. All authors read and approved the manuscript.

DECLARATION OF INTERESTS

The authors declare no competing interests.

REFERENCES

1. Locatelli, F., and Niemeyer, C.M. (2015). How I treat juvenile myelomonocytic leukemia. Blood *125*, 1083–1090.
2. Wintering, A., Dvorak, C.C., Stieglitz, E., and Loh, M.L. (2021). Juvenile myelomonocytic leukemia in the molecular era: a clinician's guide to diagnosis, risk stratification, and treatment. Blood Adv. *5*, 4783–4793.
3. Stieglitz, E., Taylor-Weiner, A.N., Chang, T.Y., Gelston, L.C., Wang, Y.D., Mazor, T., Esquivel, E., Yu, A., Seepo, S., Olsen, S., et al. (2015). The genomic landscape of juvenile myelomonocytic leukemia. Nat. Genet. *47*, 1326–1333.
4. Murakami, N., Okuno, Y., Yoshida, K., Shiraishi, Y., Nagae, G., Suzuki, K., Narita, A., Sakaguchi, H., Kawashima, N., Wang, X., et al. (2018). Integrated molecular profiling of juvenile myelomonocytic leukemia. Blood *131*, 1576–1586.
5. Locatelli, F., Nöllke, P., Zecca, M., Korthof, E., Lanino, E., Peters, C., Pession, A., Kabisch, H., Uderzo, C., Bonfim, C.S., et al. (2005). Hematopoietic stem cell transplantation (HSCT) in children with juvenile myelomonocytic leukemia (JMML): results of the EWOG-MDS/EBMT trial. Blood *105*, 410–419.
6. Guo, Y.J., Pan, W.W., Liu, S.B., Shen, Z.F., Xu, Y., and Hu, L.L. (2020). ERK/MAPK signalling pathway and tumorigenesis (Review). Exp. Ther. Med. *19*, 1997–2007.
7. Schönung, M., Meyer, J., Nöllke, P., Olshen, A.B., Hartmann, M., Murakami, N., Wakamatsu, M., Okuno, Y., Plass, C., Loh, M.L., et al. (2021). International consensus definition of DNA methylation subgroups in juvenile myelomonocytic leukemia. Clin. Cancer Res. *27*, 158–168.
8. Harder, A. (2021). MEK inhibitors - novel targeted therapies of neurofibromatosis associated benign and malignant lesions. Biomark. Res. *9*, 26–29.
9. Chang, T., Krisman, K., Theobald, E.H., Xu, J., Akutagawa, J., Lauchle, J.O., Kogan, S., Braun, B.S., and Shannon, K. (2013). Sustained MEK inhibition abrogates myeloproliferative disease in Nf1 mutant mice. J. Clin. Invest. *123*, 335–339.
10. Lyubynska, N., Gorman, M.F., Lauchle, J.O., Hong, W.X., Akutagawa, J.K., Shannon, K., and Braun, B.S. (2011). A MEK inhibitor abrogates myeloproliferative disease in Kras mutant mice. Sci. Transl. Med. *3*, 76ra27–8.
11. Stieglitz, E., Loh, M.L., Meyer, J., Zhang, C., Barkauskas, D.A., Hall, D., Fox, E., and Weigel, B.J. (2021). MEK inhibition demonstrates activity in relapsed, refractory patients with juvenile myelomonocytic leukemia: results from COG study ADVL1521. Blood *138*, 3679.
12. Niemeyer, C.M., Flotho, C., Lipka, D.B., Starý, J., Rössig, C., Baruchel, A., Klingebiel, T., Micalizzi, C., Michel, G., Nysom, K., et al. (2021). Response to upfront azacitidine in juvenile myelomonocytic leukemia in the AZA-JMML-001 trial. Blood Adv. *5*, 2901–2908.
13. Cseh, A., Niemeyer, C.M., Yoshimi, A., Dworzak, M., Hasle, H., van den Heuvel-Eibrink, M.M., Locatelli, F., Masetti, R., Schmugge, M., Groß-Wieltsch, U., et al. (2015). Bridging to transplant with azacitidine in juvenile myelomonocytic leukemia : a retrospective. Blood *125*, 2311–2313.
14. Honda, Y., Muramatsu, H., Nanjo, Y., Hirabayashi, S., Meguro, T., Yoshida, N., Kakuda, H., Ozono, S., Wakamatsu, M., Moritake, H., et al. (2022). A retrospective analysis of azacitidine treatment for juvenile myelomonocytic leukemia. Int. J. Hematol. *115*, 263–268.
15. Wei, A.H., Strickland, S.A., Hou, J.Z., Fiedler, W., Lin, T.L., Walter, R.B., Enjeti, A., Tiong, I.S., Savona, M., Lee, S., et al. (2019). Venetoclax combined with low-dose cytarabine for previously untreated patients with acute myeloid leukemia: results from a phase Ib/II study. J. Clin. Oncol. *37*, 1277–1284.
16. DiNardo, C.D., Pratz, K., Pullarkat, V., Jonas, B.A., Arellano, M., Becker, P.S., Frankfurt, O., Konopleva, M., Wei, A.H., Kantarjian, H.M., et al. (2019). Venetoclax combined with decitabine or azacitidine in treatment-naive, elderly patients with acute myeloid leukemia. Blood *133*, 7–17.
17. Kloos, A., Mintzas, K., Winckler, L., Gabdoulline, R., Alwie, Y., Jyotsana, N., Kattre, N., Schottmann, R., Scherr, M., Gupta, C., et al. (2020). Effective drug treatment identified by in vivo screening in a transplantable patient-derived xenograft model of chronic myelomonocytic leukemia. Leukemia *34*, 2951–2963.
18. Hanft, K.M., Hamed, E., Kaiser, M., Würtemberger, J., Schneider, M., Pietsch, T., Feige, U., Meiss, F., Krengel, S., Niemeyer, C., and Hettmer, S. (2022). Combinatorial effects of azacitidine and trametinib on NRAS-mutated melanoma. Pediatr. Blood Cancer *69*, 294688–e29511.
19. Jimenez-Duran, G., Luque-Martin, R., Patel, M., Koppe, E., Bernard, S., Sharp, C., Buchan, N., Rea, C., de Winther, M.P.J., Turan, N., et al. (2020). Pharmacological validation of targets regulating CD14 during macrophage differentiation. EBioMedicine *61*, 103039.
20. Zeng, Z., Lan, T., Wei, Y., and Wei, X. (2022). CCL5/CCR5 axis in human diseases and related treatments. Genes Dis. *9*, 12–27.
21. Mochizuki, S., and Okada, Y. (2007). ADAMs in cancer cell proliferation and progression. Cancer Sci. *98*, 621–628.
22. Caunt, C.J., and Keyse, S.M. (2013). Dual-specificity MAP kinase phosphatases (MKPs): shaping the outcome of MAP kinase signalling. FEBS J. *280*, 489–504.
23. Kong, T., Laranjeira, A.B.A., Yang, K., Fisher, D.A.C., Yu, L., Poittevin De La Frégonnière, L., Wang, A.Z., Ruzinova, M.B., Fowles, J.S., Fulbright, M.C., et al. (2022). DUSP6 mediates resistance to JAK2 inhibition and drives myeloproliferative neoplasm disease progression. Nat. Cancer *4*, 108–127.
24. Gao, F., and Liu, W.J. (2016). Advance in the study on p38 MAPK mediated drug resistance in leukemia. Eur. Rev. Med. Pharmacol. Sci. *20*, 1064–1070.
25. De Vries, A.C.H., Zwaan, C.M., and Van Den Heuvel-Eibrink, M.M. (2010). Molecular basis of juvenile myelomonocytic leukemia. Haematologica *95*, 179–182.
26. Harmer, D., Falank, C., and Reagan, M.R. (2019). Interleukin-6 interweaves the bone marrow microenvironment, bone loss, and multiple myeloma. Front. Endocrinol. (Lausanne). *9*, 1–15.
27. Fonte, E., Vilia, M.G., Reverberi, D., Sana, I., Scarfò, L., Ranghetti, P., Orfanelli, U., Cenci, S., Cutrona, G., Ghia, P., and Muzio, M. (2017). Toll-like receptor 9

stimulation can induce IκBζ expression and IgM secretion in chronic lymphocytic leukemia cells. Haematologica *102*, 1901–1912.

28. Xu, T., Rao, T., Yu, W.M., Ning, J.Z., Yu, X., Zhu, S.M., Yang, K., Bai, T., and Cheng, F. (2021). Upregulation of NFKBIZ affects bladder cancer progression via the PTEN/PI3K/Akt signaling pathway. Int. J. Mol. Med. *47*, 109–112.
29. Rohena-Rivera, K., Sánchez-Vázquez, M.M., Aponte-Colón, D.A., Forestier-Román, I.S., Quintero-Aguiló, M.E., Martínez-Ferrer, M., and Martanez-Ferrer, M. (2017). IL-15 regulates migration, invasion, angiogenesis and genes associated with lipid metabolism and inflammation in prostate cancer. PLoS One *12*, 01727866–e172827.
30. Shoham, N.G., Centola, M., Mansfield, E., Hull, K.M., Wood, G., Wise, C.A., and Kastner, D.L. (2003). Pyrin binds the PSTPIP1/CD2BP1 protein, defining familial Mediterranean fever and PAPA syndrome as disorders in the same pathway. Proc. Natl. Acad. Sci. USA *100*, 13501–13506.
31. Kumar, B.S., Kumar, P.S., Sowgandhi, N., Prajwal, B.M., Mohan, A., Sarma, K.V.S., and Sarma, P.V.G.K. (2016). Identification of novel mutations in CD2BP1 gene in clinically proven rheumatoid arthritis patients of south India. Eur. J. Med. Genet. *59*, 404–412.
32. Karki, R., Man, S.M., and Kanneganti, T.D. (2017). Inflammasomes and cancer. Cancer Immunol. Res. *5*, 94–99.
33. Zhong, C., Wang, R., Hua, M., Zhang, C., Han, F., Xu, M., Yang, X., Li, G., Hu, X., Sun, T., et al. (2021). NLRP3 inflammasome promotes the progression of acute myeloid leukemia via IL-1β pathway. Front. Immunol. *12*, 1–15.
34. Li, R., Ding, Z., Jin, P., Wu, S., Jiang, G., Xiang, R., Wang, W., Jin, Z., Li, X., Xue, K., et al. (2021). Development and validation of a novel prognostic model for acute myeloid leukemia based on immune-related genes. Front. Immunol. *12*, 639634–639638.
35. Cooper, J., and Giancotti, F.G. (2019). Integrin signaling in cancer: mechanotransduction, stemness, epithelial plasticity, and therapeutic resistance. Cancer Cell *35*, 347–367.
36. Hood, J.D., and Cheresh, D.A. (2002). Role of integrins in cell invasion and migration. Nat. Rev. Cancer *2*, 91–100.
37. Khurana, S., Schouteden, S., Manesia, J.K., Santamaria-Martínez, A., Huelsken, J., Lacy-Hulbert, A., and Verfaillie, C.M. (2016). Outside-in integrin signalling regulates haematopoietic stem cell function via Periostin-Itgav axis. Nat. Commun. *7*, 13500.
38. Ramdas, B., Yuen, L.D., Palam, L.R., Patel, R., Pasupuleti, S.K., Jideonwo, V., Zhang, J., Maguire, C., Wong, E., Kanumuri, R., et al. (2022). Inhibition of BTK and PI3Kδ impairs the development of human JMML stem and progenitor cells. Mol. Ther. *30*, 2505–2521.
39. Sturm, G., Finotello, F., Petitprez, F., Zhang, J.D., Baumbach, J., Fridman, W.H., List, M., and Aneichyk, T. (2019). Comprehensive evaluation of transcriptome-based cell-type quantification methods for immuno-oncology. Bioinformatics *35*, i436–i445.
40. Li, B., Severson, E., Pignon, J.C., Zhao, H., Li, T., Novak, J., Jiang, P., Shen, H., Aster, J.C., Rodig, S., et al. (2016). Comprehensive analyses of tumor immunity: implications for cancer immunotherapy. Genome Biol. *17*, 174–216.
41. Petitprez, F., Levy, S., Sun, C.M., Meylan, M., Linhard, C., Becht, E., Elarouci, N., Tavel, D., Roumenina, L.T., Ayadi, M., et al. (2020). The murine Microenvironment Cell population counter method to estimate abundance of tissue-infiltrating immune and stromal cell populations in murine samples using gene expression. Genome Med. *12*, 86.
42. Bergstraesser, E., Hasle, H., Rogge, T., Fischer, A., Zimmermann, M., Noellke, P., and Niemeyer, C.M. (2007). Non-hematopoietic stem cell transplantation treatment of juvenile myelomonocytic leukemia: a retrospective analysis and definition of response criteria. Pediatr. Pediatr. Blood Cancer *49*, 629–633.
43. Chang, T.Y., Dvorak, C.C., and Loh, M.L. (2014). Bedside to bench in juvenile myelomonocytic leukemia: insights into leukemogenesis from a rare pediatric leukemia. Blood *124*, 2487–2497.
44. Vaseva, A.V., and Yohe, M.E. (2020). Targeting RAS in pediatric cancer: is it becoming a reality? Curr. Opin. Pediatr. *32*, 48–56.
45. Cheng, Y., and Tian, H. (2017). Current development status of MEK inhibitors. Molecules *22*, 1551.
46. Yamaguchi, T., Kakefuda, R., Tajima, N., Sowa, Y., and Sakai, T. (2011). Antitumor activities of JTP-74057 (GSK1120212), a novel MEK1/2 inhibitor, on colorectal cancer cell lines in vitro and in vivo. Int. J. Oncol. *39*, 23–31.
47. Kerstjens, M., Driessen, E.M.C., Willekes, M., Pinhanços, S.S., Schneider, P., Pieters, R., and Stam, R.W. (2017). MEK inhibition is a promising therapeutic strategy for MLL-rearranged infant acute lymphoblastic leukemia patients carrying RAS mutations. Oncotarget *8*, 14835–14846.
48. Kerstjens, M., Pinhancos, S.S., Castro, P.G., Schneider, P., Wander, P., Pieters, R., and Stam, R.W. (2018). Trametinib inhibits RAS-mutant MLL-rearranged acute lymphoblastic leukemia at specific niche sites and reduces ERK phosphorylation in vivo. Haematologica *103*, e147–e150.
49. Hecht, A., Meyer, J.A., Behnert, A., Wong, E., Chehab, F., Olshen, A., Hechmer, A., Aftandilian, C., Bhat, R., Choi, S.W., et al. (2022). Molecular and phenotypic diversity of CBL- mutated juvenile myelomonocytic leukemia. Haematologica *107*, 178–186.
50. Cai, Z., Zhang, C., Kotzin, J.J., Williams, A., Henao-Mejia, J., and Kapur, R. (2020). Role of lncRNA Morrbid in PTPN11(Shp2)E76K-driven juvenile myelomonocytic leukemia. Blood Adv. *4*, 3246–3251.
51. Arora, D., Köthe, S., Van Den Eijnden, M., Hooft van Huijsduijnen, R., Heidel, F., Fischer, T., Scholl, S., Tölle, B., Böhmer, S.A., Lennartsson, J., et al. (2012). Expression of protein-tyrosine phosphatases in acute myeloid leukemia cells: FLT3 ITD sustains high levels of DUSP6 expression. Cell Commun. Signal. *10*, 19.
52. Shi, Y.Y., Small, G.W., and Orlowski, R.Z. (2006). Proteasome inhibitors induce a p38 mitogen-activated protein kinase (MAPK)-dependent anti-apoptotic program involving MAPK phosphatase-1 and Akt in models of breast cancer. Breast Cancer Res. Treat. *100*, 33–47.
53. Abrams, M.T., Robertson, N.M., Litwack, G., and Wickstrom, E. (2005). Evaluation of glucocorticoid sensitivity in 697 pre-B acute lymphoblastic leukemia cells after overexpression or silencing of MAP kinase phosphatase-1. J. Cancer Res. Clin. Oncol. *131*, 347–354.
54. Wang, Z., Xu, J., Zhou, J.Y., Liu, Y., and Wu, G.S. (2006). Mitogen-activated protein kinase phosphatase-1 is required for cisplatin resistance. Cancer Res. *66*, 8870–8877.
55. Haagenson, K.K., and Wu, G.S. (2010). The role of MAP kinases and MAP kinase phosphatase-1 in resistance to breast cancer treatment. Cancer Metastasis Rev. *29*, 143–149.
56. Xu, D., Liu, X., Yu, W.M., Meyerson, H.J., Guo, C., Gerson, S.L., and Qu, C.K. (2011). Non-lineage/stage-restricted effects of a gain-of-function mutation in tyrosine phosphatase Ptpn11 (Shp2) on malignant transformation of hematopoietic cells. J. Exp. Med. *208*, 1977–1988.
57. Ramdas, B., Mali, R.S., Palam, L.R., Pandey, R., Cai, Z., Pasupuleti, S.K., Burns, S.S., and Kapur, R. (2020). Driver mutations in leukemia promote disease pathogenesis through a combination of cell-autonomous and niche modulation. Stem Cell Rep. *15*, 95–109.
58. Dobin, A., Davis, C.A., Schlesinger, F., Drenkow, J., Zaleski, C., Jha, S., Batut, P., Chaisson, M., and Gingeras, T.R. (2013). STAR: Ultrafast universal RNA-seq aligner. Bioinformatics *29*, 15–21.
59. Liao, Y., Smyth, G.K., and Shi, W. (2014). FeatureCounts: an efficient general purpose program for assigning sequence reads to genomic features. Bioinformatics *30*, 923–930.
60. Robinson, M.D., McCarthy, D.J., and Smyth, G.K. (2010). edgeR: a Bioconductor package for differential expression analysis of digital gene expression data. Bioinformatics *26*, 139–140.
61. McCarthy, D.J., Chen, Y., and Smyth, G.K. (2012). Differential expression analysis of multifactor RNA-Seq experiments with respect to biological variation. Nucleic Acids Res. *40*, 4288–4297.
62. Dennis, G., Sherman, B.T., Hosack, D.A., Yang, J., Gao, W., Lane, H.C., and Lempicki, R.A. (2003). DAVID: database for annotation, visualization, and integrated discovery. Genome Biol. *4*, P3.
63. Huang, D.W., Sherman, B.T., and Lempicki, R.A. (2009). Systematic and integrative analysis of large gene lists using DAVID bioinformatics resources. Nat. Protoc. *4*, 44–57.
64. Subramanian, A., Tamayo, P., Mootha, V.K., Mukherjee, S., Ebert, B.L., Gillette, M.A., Paulovich, A., Pomeroy, S.L., Golub, T.R., Lander, E.S., and Mesirov, J.P. (2005). Gene set enrichment analysis: a knowledge-based approach for interpreting genome-wide expression profiles. Proc. Natl. Acad. Sci. USA *102*, 15545–15550.